Open-Loop Analysis for the Stability of Reactive Distillation Columns with Intermediate Condensers for the Production of Silane

J. Rafael Alcántara-Avila*, Julián Cabrera-Ruiz, Hao-Yeh Lee*****

** Department of Chemical Engineering, Kyoto University, Kyoto, Japan, (e-mail: jrafael@cheme.kyoto-u.ac.jp)*

*** Departamento de Ingenieria Quimica, Universidad de Guanajuato, Guanajuato, Mexico, (e-mail: j.cabreraruiz@ugto.mx)*

**** Department of Chemical Engineering, National Taiwan University of Science and Technology, Taipei, Taiwan, (e-mail: haoyehlee@mail.ntust.edu.tw)*

Abstract: The production of cost-effective Silane is paramount for reducing the cost in the solar photovoltaic industry to make it a more competitive renewable energy source. Thus, the production of Silane through reactive distillation (RD) is an alternative that reduces the equipment size, cost, and operation in comparison with a typical reaction-separation process mainly because the chemical reactions are limited by equilibrium. This work presents an open-loop analysis for RD columns with two intermediate condensers (RD-2IC) and different heat distribution in the inter condensers (IC). The open-loop stability of the RD columns analysis is done to understand the relationship between heat distribution at IC and their theoretical control properties to determine which heat distribution conditions result in stable operation. The results showed that RD-2IC columns attained economic savings compared to the RD column. Also, the optimal RD-2IC has better control properties than the RD column in an open-loop analysis.

Keywords: Reactive Distillation, Control properties, SVD, Process control, Process simulation.

1. INTRODUCTION

The use of alternative energy sources that can replace fossil fuels has been steadily increasing in the last decades. Solar photovoltaic is renewable energy, considered clean energy, because it does not release greenhouse gas emissions into the atmosphere. Therefore, solar energy has been researched widely in the last decades. In a review of solar grade silicon production (Yadav, Chattopadhyay, and Singh, 2017), it was mentioned that silicon-based modules dominate the solar photovoltaic industry.

1.1 Silicon production

The most important process to obtain solar grade silicon (SOG-Si) is the Siemens process, accounting for approximately 90% of worldwide polysilicon production (Bye and Ceccaroli, 2014). This process uses trichlorosilane (TCS) as an intermediate. At a later step, Silicon is obtained through chemical vapor decomposition (CVD) in a reactor.

The Komatsu/Union Carbide (UCC) process is the second most widely used commercial process. It utilizes the decomposition of Silane (SiH4). In this process, Silane is produced after the hydrochlorination and distillation steps by disproportionation of TCS and dichlorosilane (DCS) through catalytic redistribution (Yaws *et al.*, 1979). The resulting gases are distilled to separate Silane. Then, the Silane is thermally decomposed through a pyrolysis reaction.

Since Silane is a raw material for producing Silicon, the market demand for Silane is expected to grow rapidly following the growth of solar cell demand. In addition, Silane and chlorosilanes are essential chemicals for the production of microscopic glass slides, oxidation masks, and corrosion-resistant coating, which are used in a wide variety of innovative applications (Alcántara-Avila *et al.*, 2016).

1.2 Reactive Distillation for Silane production

Reactive Distillation (RD) is a technology that combines reaction and separation processes into a single column. Therefore, RD can overcome chemical equilibrium limitations. Thus, RD can be implemented for generating and separating Silane. The typical RD column feeds TCS as raw material. It reacts to obtain Silane as the top product and Silicon Tetra chloride (STC) as the bottom byproduct (Huang *et al.*, 2013).

1.3 Current limitations in RD for Silane production

The continuous removal of the products out from the reaction section can circumvent the conversion and phase equilibrium limitations. In the reaction section, the catalytic disproportionation of TCS to Silane occurs. Thus, RD can reduce energy consumption and investment cost compared to the conventional process. However, there is still the need to use expensive refrigerants to condense Silane at the top of the RD column, which has a low boiling temperature (-112 ºC) at normal pressure. Since using refrigerants in cryogenic conditions are very expensive, current RD technology results in an expensive process.

In order to reduce the use of an expensive refrigerant at the top condenser, the use of intermediate condensers (IC), which can be installed at the stages of an RD column, has been proposed

(Huang *et al.*, 2013). Since the temperature at stages is higher than that at the condenser, less expensive utilities can be used to condense some of the vapor going towards the condenser. Previous research has done the design and control of several RD columns with one or two IC (Lee *et al.*, 2022). Among the solutions with two ICs, a set of designs with similar costs were obtained. The principal difference between designs is the heat load distribution at the ICS. Thus, this work studies the control properties through an open-loop analysis based on the singular value decomposition (SVD) for designs with different heat load distribution to know if the optimal steady-state design is also the one with the best control properties.

1.4 Tradeoff between optimality and controllability

Luyben presented a comparison between extractive distillation (ED), pressure swing distillation (PSD), and a single refrigerated distillation (SRD) for the separation of n-heptane and iso-butanol. PSD has the highest cost and the most complex design and operation. ED attained the lowest cost, but its dynamic performance is not as good as that of SRD despite its high cost (Luyben, 2017). Therefore, in some cases, the steady-state design with the lowest cost does not necessarily guarantee the best dynamic performance. Therefore, it is necessary to integrate both design and control simultaneously or to develop more appropriate optimization strategies to improve the conventional "control after design" sequence so that the tradeoff between steady-state design and dynamic simulation can be assessed (Alcantara-Avila *et al.*, 2021).

The simultaneous design and control of distillation processes can be classified into controllability index-based approaches, mixed-integer nonlinear dynamic optimization (MIDO) problems, robust-based approaches, embedded control optimizations, and black-box optimization approaches. However, the most common challenges in integrating design and control are related to uncertainty and disturbances, multiple conflicting objectives, problem size, handling integer variables, and the balance between local and global optimality (Rafiei and Ricardez-Sandoval, 2020). Thus, there are a few open questions and challenges that require further investigation.

1.5 Open-loop based controllability index

Typically, the close-loop controllability is evaluated after a process has been designed. However, when there are several alternative processes, the open-loop controllability analysis is done to fast-screen them to perform closed-loop analysis only to the most promising choice. The simultaneous design and control of distillation processes have been researched in a multi-objective optimization framework in which an open-loop based controllability index has been considered as objective for example in the reaction for the of furfural (Romero-García *et al.*, 2020), and reactive distillation processes to produce diphenyl carbonate (Contreras-Zarazúa *et al.*, 2017). Also, an open-loop based controllability index has been embedded in a global stochastic optimization framework to simultaneously evaluate the design and control of reactive distillation processes (Cabrera-Ruiz *et al.*, 2017) and thermally coupled processes (Cabrera-Ruiz et al., 2018).

In this work, a controllability index-based approach was taken. Firstly, the control properties of RD columns were evaluated using only steady-state information to screen the most promising alternatives, then, for the chosen alternatives, the control properties in the frequency domain were evaluated.

2. STEADY-STATE OPTIMIZATION

In previous research (Lee *et al.*, 2022), the design and control of several RD columns with one and two ICs were studied. The design and optimization of the RD column without any ICs were done through a global-search randomized method based on a Simulated Annealing Algorithm (SAA). The optimization variables of the RD column are the number of stages in the rectifying section (N_r), reaction section (N_{rxn}), and stripping section (N_s), the feed stage (N_f), and the column pressure (P). In addition, for RD-2IC the optimization variables are the locations of intermediate condensers (L_{1IC} and L_{2IC}) and heat removal of intermediate condensers (Q_{1IC} and Q_{2IC}). The Total Annual Cost (TAC) defined by (1) was minimized for RD and RD-2IC.

$$TAC = CAP/PBP + OPT \tag{1}$$

where CAP is the capital cost, which includes the cost of the column, trays, and heat exchangers (i.e., condenser, intermediate condensers, and reboiler). OPT is the operating cost, which includes the cost of cooling and heating utilities and catalyst. PBP is the payback period, which was three years.

2.1 Optimization of the RD column

The RD column was optimized using a Simulated Annealing Algorithm (SAA) and solved by combining Aspen Plus V10.0 and MATLAB R2019B. The RD-2IC was optimized by an iterative simulation-optimization algorithm (Alcántara-Avila *et al.*, 2016). Figure 1 shows the design of the RD column.

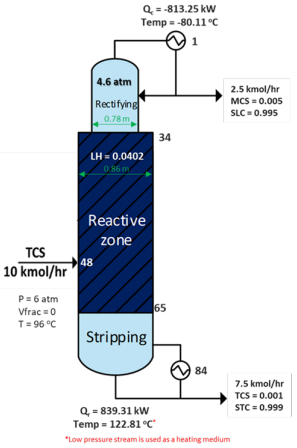

Figure 1. RD column base design

2.2 Optimization of RD-2IC columns

The design of RD-2IC columns was obtained after solving an iterative simulation-optimization solution procedure adopted from previous research (Alcántara-Avila *et al.*, 2016). At the simulation step, all nonlinear equations (e.g., complex thermodynamic relationships) and non-convex equations (e.g.,

bilinear terms of the product between flows and compositions) are handled. In contrast, at the optimization step, a combinatorial problem is solved to find the best locations of stages and their heat loads by minimizing the OPT. Since distillation is dominated mainly by the operation cost, especially when expensive utilities are used, it is reasonable to choose the OPT minimization as the objective function. The simulation and optimization software are linked through an interface programmed in Microsoft VBA. The simulation step was done in Aspen Plus V10.0, while the optimization step was done in CPLEX Optimization Studio 12.8 through the formulation of a mixed-integer linear programming (MILP) problem.

The optimization of RD-2IC columns was represented by a superstructure between heat sinks (i.e., stages in the rectifying section) and heat sources (i.e., refrigerant and cooling utilities). The superstructure was reformulated as a MILP problem. The objective function in the mathematical model is the minimization of OPT while energy balances at each stage in the rectifying section, heat exchange feasibility and connectivity expressions are the constraints (Lee et al., 2022). The relationship between energy removed at stages and the changes is reboiler and condenser duty can be approximated by piece-wise linear functions (Alcántara-Avila, Hasebe and Kano, 2013). Thus, all the equations are linear.

RD-2IC columns were optimized by limiting the maximum allowed heat removal ($Q_{IC}^{\max}$) at heat exchangers between 704 kW and 384 kW. This was done because there is no *a priori* information about the optimal heat removal value. Figure 2a shows a suboptimal RD-2IC column (i.e., RD-2IC$_{704}$), and Fig. 2b shows the optimal RD-2IC column (i.e., RD-2IC$_{384}$).

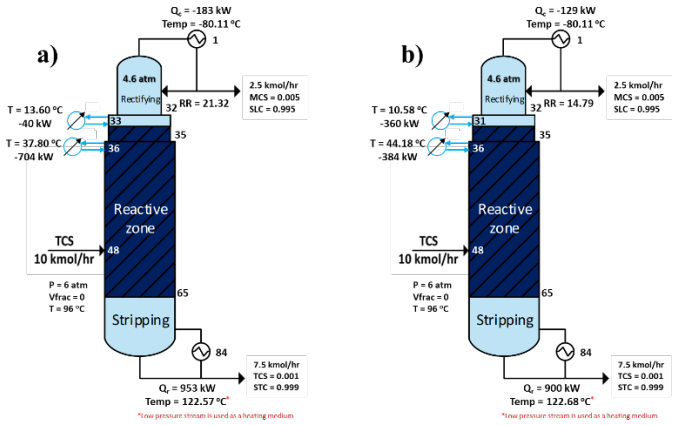

Figure 2. RD-2IC solutions: suboptimal process (left) and optimal process (right)

Figure 3 shows the TAC for several values of $Q_{IC}^{\max}$. It was observed that a set of optimal RD-2IC columns could be obtained by constraining $Q_{1IC} \leq Q_{IC}^{\max}$ and $Q_{2IC} \leq Q_{IC}^{\max}$ during the optimization step. The subscripts in RD-2IC mean the value of $Q_{IC}^{\max}$ at which optimizations were done.

When the maximum heat removal is reduced, a set of several solutions was obtained. There is an optimality gap of 6 % among the solutions between the designs of Fig. 2a and Fig. 2b. Details about the optimization procedure and designs of all RD-2IC columns can be found in (Lee et al., 2022).

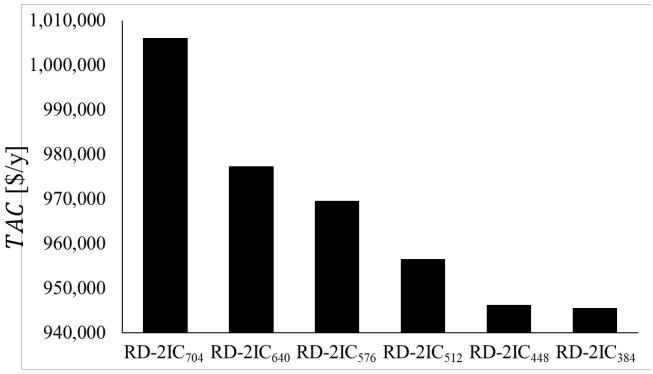

Figure 3. Relationship between TAC and $Q_{IC}^{\max}$ for the obtained RD-2IC solutions

Therefore, in this work, the following questions arise, *is there a tradeoff between TAC and controllability? Does the heat load significantly affect the control properties of the system?* To answer these questions, an open-loop analysis was done for the obtained designs.

3. OPEN-LOOP ANALYSIS

As explained in Section 1.5, an open-loop based controllability index based on the Singular Value Decomposition (SVD) method can be incorporated during optimization or post-optimization. This section shows the procedure to perform open-loop analysis.

This work studied a system of four inputs and two outputs. Therefore, the SVD method can evaluate real and complex matrices that can be square or non-square over a range of frequencies or just at zero frequency. Similarly, the Morari resiliency index (MRI) can be used to give some guidance in choosing the best set of manipulated variables. The MRI is the minimum singular value of the process open-loop transfer function matrix, which is indirectly evaluated in this work (Luyben, 1992).

Additionally, the stability of loop pairing can be analyzed by the Niederlinski index (NI) and the relative gain array (RGA), which are applied for 2x2 matrices or square matrices, respectively. The NI simply finds unpaired loop gains effect and compares that with paired loop gains effect. If the unpaired loop gain is higher than paired loop gain, then the stability of loop pairing is poor, which can be indicated by a negative value of NI. If the NI value is positive, loop pairing is good (Lakshmanaprabu, Banu and Karthik, 2015). In the RGA method, values close to unity in the diagonal and close to zero in the off-diagonal should be chosen because they imply minimal interactions between the control loops and facilitate efficient disturbance rejection (Iftakher *et al.*, 2021).

Although some controllability indexes such as RGA, MRI, NI, SVD can easily be computed, they may be inaccurate since they rely on steady-state and/or dynamic linear process models, which may not capture the true process (nonlinear) dynamics especially in processes involving chemical reaction (Gutierrez *et al.*, 2014). Therefore, to overcome the limitation of the proposed SVD analysis, a closed-loop analysis is necessary.

3.1 Analysis at zero-frequency

The design of RD-2IC columns is more complex than that of the RD column. Therefore, it is important to assess their theoretical control properties at an early design stage, corresponding to an analysis at zero frequency (Miyazaki *et al.*, 2014). Table 1 shows the control variables y and manipulated variables u.

Table 1. Transfer function matrix for the optimal solution

Variable	Description, units
y_1	Silane more purity (x_{SIL}), (-)
y_2	STC more purity (x_{STC}), (-)
u_1	Reflux ratio (RR), (-)
u_2	Reboiler duty (Q_{reb}), (kW)
u_3	Heat removal at the first IC (Q_{IC1}), (kW)
u_4	Heat removal at the second IC (Q_{IC2}), (kW)

The steady-state gain between the controlled variable y_i and the manipulated variable u_j is K_{ij}, which is defined by equation (2).

$$K_{ij} = \frac{y_i(t=\infty) - y_i(t=0)}{\delta u_j/2} \tag{2}$$

where $y_i(t=0)$ is the existing steady-state and $y_i(t=\infty)$ is the new steady-state after u_j is perturbed by δ, then this value is divided by two because it is assumed that the associated valve to the manipulated value is 50% open. In this work, the manipulated variables are perturbed by 1 % ($\delta = 0.01$).

3.2 Sensitivity analysis

Since the resulting system has four inputs and two outputs, a preliminary sensitivity analysis of manipulating variables was done. The reflux rate and the reboiler duty were the most sensitive variables causing the most significant deviation in molar purity. Therefore, a reduced system of two inputs and two outputs was studied.

The control properties were evaluated at open-loop by analyzing the changes in the output variables (i.e., x_{SIL} and x_{STC}) after perturbating the input variables (i.e., RR and Q_{reb}) +0.25 %.

3.3 Singular Value Decomposition (SVD) analysis

After calculating all K_{ij} values, the resulting matrix K is factorized into three matrices using the Single Value Decomposition (SVD) method as shown in equation (3).

$$K = U\Sigma V^T \tag{3}$$

where U is the matrix of the *left singular vectors* of K and V^T is that of the *right singular vectors* of K. U and V are orthonormal or unitary eigenvectors. Σ is a real diagonal matrix containing the singular values. The diagonal elements are the singular values of K; these values are the positive roots of the eigenvalues of $K^T K$. By applying the properties of unitary matrices, equation (3) can be rewritten as Equation (4)

$$U^T y = \Sigma V^T u \tag{4}$$

where the new output is $\eta = U^T y$ and the new input is $\mu = V^T u$ so that the process model becomes $\eta = \Sigma\mu$. Because Σ is diagonal, the system of new input and output is completely decoupled at steady-state (Ogunnaike and Ray, 1994).

It is desirable to screen out unfavorable designs and control structures in the early design stage. From the control viewpoint, the minimum singular value ($\sigma_{\min}$), the maximum singular value ($\sigma_{\max}$), and the condition number ($\gamma = \sigma_{\max}/\sigma_{\min}$) are of paramount importance. $\sigma_{\min}$ implies an upper bound on the disturbance size, which the closed-loop control structure can handle. Therefore, large values over a wide range of frequencies are preferable. Contrarily, small values of γ over a wide frequency range are preferable because better closed-loop performance can be realized, even when modeling errors are present (Shimizu and Matsubara, 1985).

3.1 Analysis in the frequency domain

The steady-state designs were simulated in Aspen Plus V11.0, and then they were exported to Aspen Plus Dynamics V11.0 to execute dynamic simulations. The control variables are x_{SIL} and x_{STC}, while the manipulation variables are RR and Q_{reb}. The nominal values of x_{SIL} and x_{STC} are 0.995 and 0.999.

Dynamic simulations were executed in the time domain ($G(t)$). Therefore, their dynamic responses were transformed to the Laplace domain ($G(s)$) and then to the frequency domain ($G(j\omega)$).

4. RESULTS AND DISCUSSION

4.1 Open-loop results at zero frequency

Table 2 shows the values of $\sigma_{\min}$ and γ for the RD and RD-2IC columns at zero frequency. The subscripts in the RD-2IC columns represent the upper limit of the heat removal at intermediate condensers in kW.

Table 2. results at zero frequency

Design	γ	$\sigma_{\min}$
RD	19.95	0.04
RD-2IC$_{704}$	2.48	3.49
RD-2IC$_{640}$	52.95	1.14
RD-2IC$_{576}$	672.35	0.15
RD-2IC$_{512}$	661.39	0.15
RD-2IC$_{448}$	4.07	2.31
RD-2IC$_{384}$	2.10	3.13

From the results in the table, the RD column had values worse than RD-2IC$_{704}$ and RD-2IC$_{384}$. For this first observation, it can be concluded that the use of intermediate condensers can effectively reduce the TAC in reactive distillation processes, and they can have even better controllability. However, the values of $\sigma_{\min}$ and γ is those RD-2IC columns are not different. Therefore, the following section shows a complete comparison in the frequency domain.

4.2 open-loop results

Table 3 shows the process transfer function matrix K for the optimal process, while Table 4 shows it for the suboptimal process. The transfer functions represent the linearized model of the output responses with respect to the input variables through a perturbation of a linear system in the Laplace domain.

The transfer functions can be of first order, second order, or any combination that minimizes the error of the fitted data. The transfer functions for RD-2IC$_{384}$ have high gains and exhibit second-order responses for x_{SIL} with dead time for x_{STC}. In contrast, the transfer functions for RD-2IC$_{704}$ have small gains and exhibit second-order responses for x_{SIL} and first-order responses for x_{STC}. By looking at the matrices in Figures 3 and 4, it can be seen that RD-2IC$_{384}$ can amplify the disturbances.

From Tables 3 and 4, it can be observed that the optimal process has significant gains, which implies that the system can have large deviations in the purity of the products. Contrarily, the suboptimal process has small gains, which implies that the system can have small deviations in the purity of the products. Further analysis in the frequency domain compares both processes qualitatively.

Table 3. Transfer function matrix for RD-2IC$_{384}$

	RR	Q_{reb}
x_{SIL}	$\dfrac{-796}{0.378s^2+0.615s+1}$	$\dfrac{-796}{0.297s^2+0.545s+1}$
x_{STC}	$\dfrac{-22.187e^{-0.46s}}{0.40s+1}+\dfrac{22.986}{0.303s^2+0.55s+1}$	$\dfrac{-3.791e^{-0.32s}}{0.38s+1}+\dfrac{4.59}{0.336s^2+0.58s+1}$

Table 4. Transfer function matrix for RD-2IC$_{704}$

	RR	Q_{reb}
x_{SIL}	$\dfrac{0.895}{0.007s^2+0.087s+1}$	$\dfrac{-5.753}{0.006s^2+0.068s+1}$
x_{STC}	$\dfrac{-0.028}{4.858s+1}$	$\dfrac{0.3178}{7.419s+1}$

The frequency (ω) was varied from 0.0001 to 10,000. Figure 4 shows the condition number for the RD-2IC columns in Fig. 2, while Figure 5 shows the minimum singular value for the RD-2IC columns in Fig. 2.

At low frequencies ($\omega < 0.1$) and high frequencies ($\omega > 100$), RD-2IC$_{384}$ has γ values smaller than those for RD-2IC$_{704}$. However, at frequency values around 1 to 100, RD-2IC$_{704}$ has γ values smaller than those for RD-2IC$_{384}$. Similarly, at low frequencies ($\omega < 0.1$) and frequencies ($\omega > 100$), RD-2IC$_{384}$ has $\sigma_{\min}$ values higher than those for RD-2IC$_{704}$. However, at frequency values around 1 to 100, RD-2IC$_{704}$ has $\sigma_{\min}$ values higher than those for RD-2IC$_{384}$.

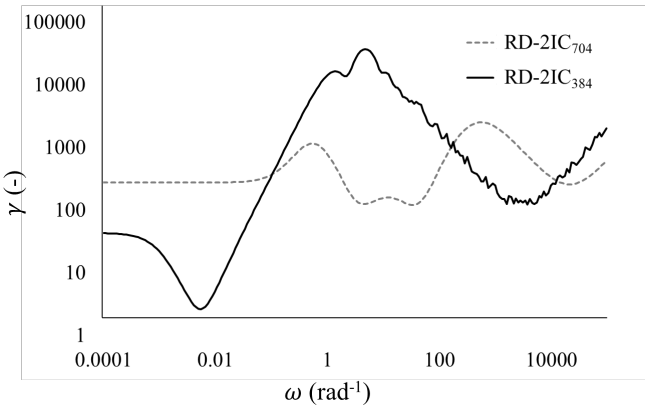

Figure 4. Condition number for the compared RD-2IC$_{384}$ processes

Considering that high-frequency values ($\omega > 100$) lack realistic physical sense (Morari and Zafiriou, 1989; Cabrera-Ruiz *et al.*, 2017), it can be concluded that at low frequencies ($\omega < 0.1$) RD-2IC$_{384}$ not only resulted in the most economical process, but also in the one with the best controllability at low frequencies. However, at moderate frequencies ($1 < \omega < 100$), there is a tradeoff between TAC and controllability between RD-2IC$_{704}$ and RD-2IC$_{384}$.

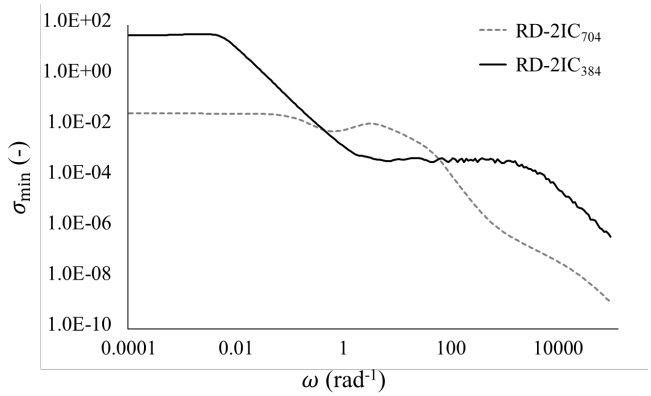

Figure 5. Minimum Singular Value for the compared RD-2IC$_{384}$ processes

6. CONCLUSIONS

This work presented an open-loop analysis to compare reactive distillation columns with two intermediate condensers. The alternatives were optimized at the steady-state in terms of Total Annual Cost. The optimal solution had a similar heat load distribution in the two intermediate condensers, while the heat load distribution in the suboptimal solution was dominant for the second intermediate condenser located at stage 36. Then, an open-loop dynamic analysis was done using the Singular Value Decomposition method at zero frequency and in the frequency domain. The comparison of results showed that at low frequencies ($\omega < 1$), the optimal solution had the best control properties, while at higher frequencies ($1 < \omega < 100$), the suboptimal solution had the best control properties. Therefore, depending on the operation frequency of the process, a tradeoff may exist between steady-state optimality and dynamic state operability.

REFERENCES

Alcantara-Avila, J. R. *et al.* (2021) “Advancements in Optimization and Control Techniques for Intensifying Processes,” *Processes*, 9(12), 2150. doi:10.3390/pr9122150.

Alcántara-Avila, J. R. *et al.* (2016) “Design of a Multitask Reactive Distillation with Intermediate Heat Exchangers for the Production of Silane and Chlorosilane Derivates,” *Industrial and Engineering Chemistry Research*, 55(41), 10968−10977. doi:10.1021/acs.iecr.6b02277.

Alcántara-Avila, J. R., Hasebe, S. and Kano, M. (2013) “New synthesis procedure to find the optimal distillation sequence with internal and external heat integrations,” *Industrial and Engineering Chemistry Research*, 52(13), 4851–4862. doi:10.1021/ie302863p.

Bye, G. and Ceccaroli, B. (2014) “Solar grade silicon: Technology status and industrial trends,” *Solar Energy Materials and Solar Cells*. Elsevier, 130, 634–646. doi:10.1016/j.solmat.2014.06.019.

Cabrera-Ruiz, J. *et al.* (2017) “Open-loop based controllability criterion applied to stochastic global optimization for intensified distillation sequences,” *Chemical Engineering Research and Design*, 123, 165–179. doi:10.1016/j.cherd.2017.05.006.

Contreras-Zarazúa, G. *et al.* (2017) “Multi-objective optimization involving cost and control properties in reactive distillation processes to produce diphenyl carbonate,” *Computers and Chemical Engineering*, 105, 185–196. doi:10.1016/j.compchemeng.2016.11.022.

Gutierrez, G. *et al.* (2014) “An MPC-based control structure selection approach for simultaneous process and control design,” *Computers and Chemical Engineering*. Elsevier Ltd, 70, 11–21. doi:10.1016/j.compchemeng.2013.08.014.

Huang, X. *et al.* (2013) “Reactive distillation column for disproportionation of trichlorosilane to silane: Reducing refrigeration load with intermediate condensers,” *Industrial and Engineering Chemistry Research*, 52(18), 6211–6220. doi:10.1021/ie3032636.

Iftakher, A. *et al.* (2021) “Integrated design and control of reactive distillation processes using the driving force approach,” *AIChE Journal*, 67(6), 1–16. doi:10.1002/aic.17227.

Lakshmanaprabu, S. K., Banu, U. S. and Karthik, D. (2015) “Real-Time Implementation of Multi-loop Internal Model Controller for Two Interacting Conical Tank Process,” in *2015 International Conference on Innovations in Information, Embedded and Communication Systems (ICIIECS)*. IEEE, 1–6. doi:10.1109/ICIIECS.2015.7193213.

Lee, H.-Y. *et al.* (2022) “Comparison of Optimization Methods for the Design and Control of Reactive Distillation with Inter Condensers,” *Computers & Chemical Engineering*.

Liang, J. *et al.* (2021) “Comparison of dynamic performances for heat integrated reactive distillation considering safety,” *Chemical Engineering and Processing - Process Intensification*. Elsevier B.V., 160, 108294. doi:10.1016/j.cep.2020.108294.

Luyben, W. L. (1992) *Practical distillation control*, *Van Nostrand Reinhold*. New York, USA. doi:10.1007/978-1-4757-0277-4.

Luyben, W. L. (2017) “Design and Control Comparison of Alternative Separation Methods for n -Heptane / Isobutanol,” *Chemical Engineering & Technology*, 40(10), 1895–1906. doi:10.1002/ceat.201600576.

Miyazaki, A. *et al.* (2014) “Trade-off assessment between controllability and energy savings in internally and externally heat integrated distillation structures,” in *5th International Symposium on Advanced Control of Industrial Processes, AdCONIP 2014*. Hiroshima.

Morari, M. and Zafiriou, E. (1989) *Robust process control*. Prentice Hall.

Ogunnaike, B. A. and Ray, H. W. (1994) *Process Dynamics, Modeling, and Control*. New York, USA: Oxford University Press.

Rafiei, M. and Ricardez-Sandoval, L. A. (2020) “New frontiers, challenges, and opportunities in integration of design and control for enterprise-wide sustainability,” *Computers and Chemical Engineering*. 132, 106610. doi:10.1016/j.compchemeng.2019.106610.

Romero-García, A. G. *et al.* (2020) “Simultaneous Design and Controllability Optimization for the Reaction Zone for Furfural Bioproduction,” *Industrial and Engineering Chemistry Research*, 59(36), 15990–16003. doi:10.1021/acs.iecr.0c02261.

Shimizu, K. and Matsubara, M. (1985) “Singular value analysis for the robust system design of distillation systems,” *Journal of Chemical Engineering of Japan*, 18(6), 525–533.

Yadav, S., Chattopadhyay, K. and Singh, C. V. (2017) “Solar grade silicon production: A review of kinetic, thermodynamic and fluid dynamics based continuum scale modeling,” *Renewable and Sustainable Energy Reviews*. 78, 1288–1314. doi:10.1016/j.rser.2017.05.019.

Yaws, C. L. *et al.* (1979) “New technologies for solar energy silicon: Cost analysis of UCC Silane Process,” *Solar Energy*, 22(6), 547–553. doi:10.1016/0038-092X(79)90027-6.